phosphate-buffered saline (150 mol L^{-1} NaCl, 3 mmol L^{-1} KCl, and 5 nmol L^{-1} phosphate; pH 7.4, 4°C). The brain was quickly removed and divided into four parts: the cerebral cortex, cerebellum, hypothalamus, and brainstem. All tissues were homogenized in 1.15% KCl (pH 7.4), 0.4% sodium dodecyl sulfate, and 7.5% acetic acid adjusted to pH 3.5 with NaOH. Thiobarbituric acid (0.3%) was added to the homogenate. The mixture was maintained at 5°C for 60 minutes, followed by heating to 100°C for 60 minutes. After cooling, the mixture was extracted using distilled water and *n*-butanolpyridine (15:1) and centrifuged at 1600 × *g* for 10 minutes. The absorbance of the organic phase was measured at 532 nm, and the amount of thiobarbituric acid reactive substances (TBARS) was determined by absorbance (17).

Statistical Analysis

All values are expressed as the mean ± SEM. Two-way repeated measures analysis of variance with Bonferroni post hoc tests was used to compare SBP and HR between groups. One-way analysis of variance with Bonferroni post hoc tests was used to compare UNE, ESR signal decay rate, and TBARS levels between groups. Differences were considered to be statistically significant for $P < .05$.

RESULTS

BP, HR, and UNE Levels

SBP was markedly decreased in OLM/AZ and CAN/AM groups after treatment for 30 days (Figure 1). Although the decreases in BP after 30 days of treatment were not different between the OLM/AZ and CAN/AM groups, OLM/AZ decreased BP more slowly than CAN/AM. In both treated groups, HR was significantly lower compared with the untreated group (Figure 1); however, the HR in OLM/AZ-treated SHRSP was significantly lower than that in the CAN/AM-treated SHRSP. UNE excretion was significantly lower in the OLM/AZ group than in the untreated group ($n = 8$ for each, $P < .05$) or before treatment group ($n = 8$ for each, $P < .05$), but was not significantly different between the CAN/AM and untreated groups (Figure 2). In addition, when changes in UNE from baseline between OLM/AZ and CAN/AM groups were compared, the changes were found to be greater in the OLM/AZ group than in the CAN/AM group (−0.32 ± 0.05 vs. −0.11 ± 0.04 μg $24\ h^{-1}$, $n = 4$ for each, $P < .05$).

Oxidative Stress in the Whole Brain as Measured Using In Vivo ESR

The signal decay rates in the whole brain were significantly decreased in both the OLM/AZ and CAN/AM groups compared with the untreated or before treatment groups (Figure 3). Decreases in the signal decay rate did not differ between the OLM/AZ and CAN/AM groups.

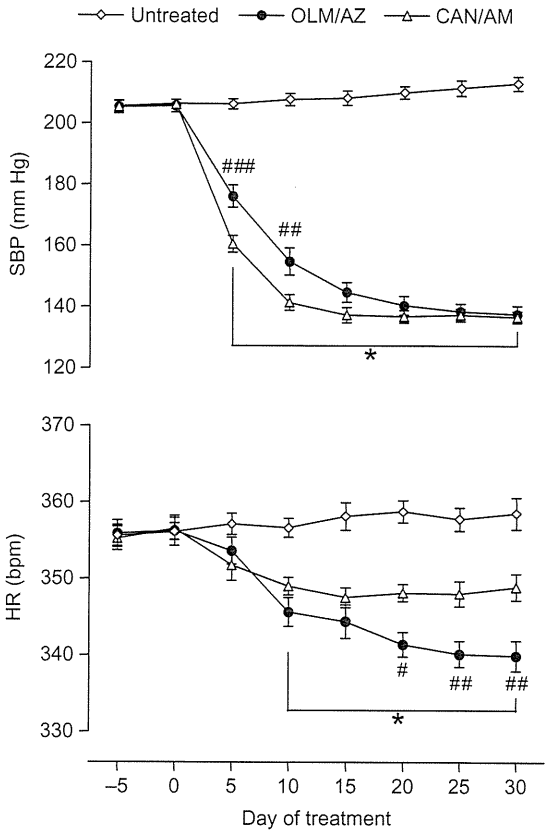

Figure 1. The effect of combination therapies of olmesartan/azelnidipine (OLM/AZ) and candesartan/amlodipine (CAN/AM) on systolic blood pressure (SBP) and heart rate (HR). Time courses of SBP and HR in the groups during the study period. $^{*}P < .001$ versus untreated group for both OLM/AZ and CAN/AM groups; $^{\#}P < .05$, $^{\#\#}P < .01$, $^{\#\#\#}P < .001$ versus CAN/AM group.

TBARS Levels in the Brain

Figure 4 shows TBARS levels in each region of the brain. In the cerebral cortex, cerebellum, and hypothalamus, TBARS levels were significantly lower in both the OLM/AZ and CAN/AM groups compared with the untreated or before treatment groups. However, in the brainstem, TBARS levels were significantly lower only in the OLM/AZ group relative to the untreated group ($n = 8$ for each, $P < .05$) or before treatment group ($n = 8$ for each, $P < .05$) and were not significantly altered in the CAN/AM group compared with the untreated group or before treatment group.

DISCUSSION

The effects of oral treatment using an OLM/AZ combination and CAN/AM combination for 30 days on the BP, HR, sympathetic activity, and brain oxidative stress in SHRSP were investigated. Major findings of

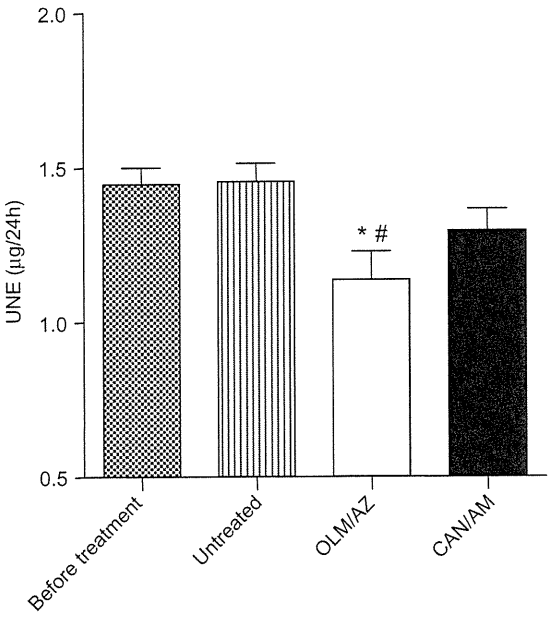

Figure 2. The effect of combination therapies of olmesartan/azelnidipine (OLM/AZ) and candesartan/amlodipine (CAN/AM) on urinary norepinephrine (UNE) excretion for 24 hours. UNE excretion as an indicator of sympathetic activity was significantly lower only in the OLM/AZ group compared with the untreated or before treatment groups. $^{*}P < .05$ versus before treatment group; $^{\#}P < .05$ versus untreated group.

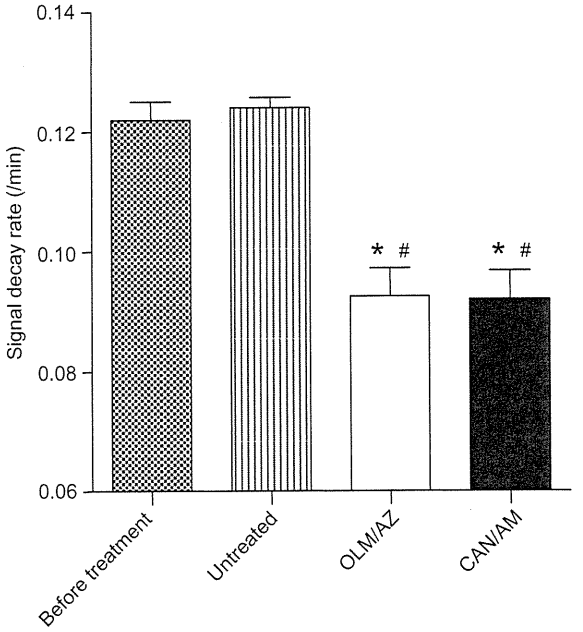

Figure 3. The effect of combination therapies of olmesartan/azelnidipine (OLM/AZ) and candesartan/amlodipine (CAN/AM) on in vivo electron spin resonance (ESR) signal decay rates. In vivo ESR signal decay rate was significantly lower in both the OLM/AZ and CAN/AM groups than in untreated or before treatment groups. $^{*}P < .001$ versus before treatment group; $^{\#}P < .001$ versus untreated group.

this study were as follows: (i) combination therapy of either OLM/AZ or CAN/AM markedly decreased BP and did not elicit a baroreflex-mediated increase in HR and sympathetic activity; (ii) OLM/AZ and CAN/AM reduced oxidative stress in the brain; and (iii) OLM/AZ, not CAN/AM, significantly decreased sympathetic activity and oxidative stress in the brainstem. These results suggest that both OLM/AZ and CAN/AM combination therapies have a powerful antihypertensive effect and do not elicit a baroreflex-mediated increase in

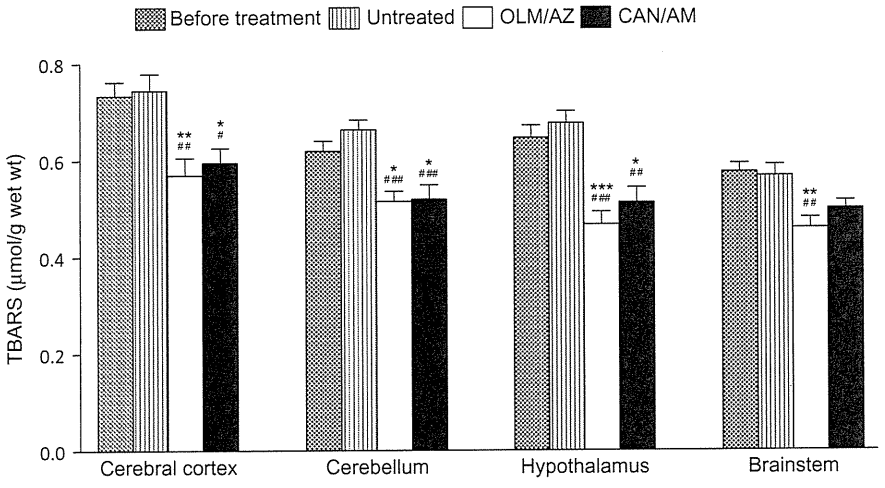

Figure 4. The effect of combination therapies of olmesartan/azelnidipine (OLM/AZ) and candesartan/amlodipine (CAN/AM) on the levels of thiobarbituric acid reactive substances (TBARS) in the brain (cerebral cortex, cerebellum, hypothalamus, and brainstem). In the cerebral cortex, cerebellum, and hypothalamus, TBARS levels were significantly lower in both the OLM/AZ and CAN/AM groups compared with the untreated or before treatment groups. In the brainstem, however, TBARS levels were significantly lower only in the OLM/AZ group compared with the untreated or before treatment groups. $^{*}P < .05$, $^{**}P < .01$, $^{***}P < .001$ versus before treatment group; $^{\#}P < .05$, $^{\#\#}P < .01$, $^{\#\#\#}P < .001$ versus untreated group.

HR or activate the sympathetic nervous system associated with an antioxidant action in the brain. Particularly, combination therapy using OLM/AZ inhibited the sympathetic activity, probably due to a greater antioxidant effect in the brainstem.

In this study, combination therapy using either OLM/AZ or CAN/AM in SHRSP markedly decreased BP considering the antihypertensive effect of each drug alone. For example, previous studies have shown that each of these combination therapies showed a stronger antihypertensive effect compared with monotherapy (24,25). In this study, despite significant reductions in BP, OLM/AZ and CAN/AM did not elicit a baroreflex-mediated increase in HR and sympathetic activity; in fact, these treatments decreased HR. The authors' group as well as other groups have previously showed that treatment using OLM, AZ, and AM did not increase the HR and/or sympathetic activity in SHRSP or spontaneously hypertensive rats (SHR) (7,12,20,26,27). Additionally, CAN did not elicit reflex tachycardia and sympathoexcitation in diabetic hypertensive rats (28). Activation of the sympathetic nervous system has an important role in hypertension pathogenesis (4); therefore, both OLM/AZ and CAN/AM are beneficial for treating hypertension because of their significant BP-lowering effect without causing sympathoexcitation.

OLM/AZ and CAN/AM reduced oxidative stress in the brain of SHRSP in this study. By measuring in vivo ESR signal decay rates in the brain and TBARS levels in several brain regions, it was confirmed that OLM/AZ and CAN/AM decreased oxidative stress in the brain. It has been previously demonstrated that the in vivo ESR method is useful for noninvasively evaluating the effect of antihypertensive drugs on brain oxidative stress in a hypertensive rat model (7). Several reports have supported the authors' finding that ARBs and CCBs exhibit antioxidant action in the brain. First, activation of angiotensin type 1 (AT1) receptors by angiotensin II (Ang II) results in ROS production. Ang II binds AT_1 receptors, activating the nicotinamide adenine dinucleotide phosphate (NAD(P)H) oxidase/Rac1 pathway, which produces superoxides in the brain (15,19). Chronic oral treatment with OLM and CAN, respectively, abolished the pressor effect of Ang II in the rostral ventrolateral medulla (RVLM) of the brainstem, where the vasomotor center is located (29), in SHR (27,30). In other studies, chronic oral treatment with OLM or CAN decreased oxidative stress in the brain in SHRSP and in salt-loaded SHRSP (7,31), respectively. Second, regarding the involvement of calcium channels in ROS generation, L-type CCBs, such as AZ and AM, can scavenge free radicals and donate protons to stabilize free electrons (32). Calcium overload, particularly in the mitochondria, generates free radicals (33). A recent study suggested that in the brain, AZ and AM reduced calcium overload and consequent oxidative stress in the neurons (34). It has been previously showed that chronic oral treatment with AZ and AM reduces oxidative stress in the brains of SHRSP (12,20) and that AZ activates copper/zinc-dependent superoxide dismutase and manganese-dependent superoxide dismutase in the RVLM of SHRSP (12). Oxidative stress in the brain, particularly in the autonomic nuclei, such as the paraventricular nucleus of the hypothalamus, nucleus tractus solitarus, and RVLM of the brainstem, contributes to the neural mechanism of hypertension (8,9,15–18). The findings of this study suggest that OLM/AZ and CAN/AM may affect the brain, thereby inhibiting the sympathetic activity, at least in part, by reducing oxidative stress in the brain, including the autonomic nuclei of the brain (8,9,15–18).

The differences in the sympathoinhibitory effect between combinations of OLM/AZ and CAN/AM were shown in this study. OLM/AZ, but not CAN/AM, significantly decreased UNE, a marker of sympathetic activity. This might have resulted from the differences in the antioxidant effect in the brainstem between OLM/AZ and CAN/AM combinations. Compared with the untreated or before treatment groups, TBARS levels in the cerebral cortex, cerebellum, and hypothalamus were significantly lower in both the OLM/AZ and CAN/AM groups; however, TBARS levels in the brainstem were significantly lower only in the OLM/AZ group. It was also demonstrated that reducing oxidative stress in the brainstem and/or hypothalamus of hypertensive rats decreased sympathetic activity, thereby reducing BP (8,9,15–18). Thus, a greater antioxidant effect of OLM/AZ on the brain, including the brainstem, compared with CAN/AM, might inhibit the sympathetic nervous system.

The extent of the actions of the ARBs and CCBs within the brain is partially dependent on the lipophilicity and pharmacokinetics of these drugs (26,35,36). Although OLM, AZ, and AM exhibit lipophilic properties (32,37), CAN exhibits a hydrophilic property. Additionally, AZ is more lipophilic than AM (32). Thus, OLM/AZ may be more beneficial for acting on the brainstem than CAN/AM because of its higher blood–brain barrier permeability. Furthermore, other mechanisms, such as active transport of the drugs through the blood–brain barrier, should be considered (38) because CAN, a hydrophilic ARB, also acts within the brain (38,39). Additionally, the disruption of the blood–brain barrier of SHRSP may affect the effect of the drugs on the brainstem (40). Further study is necessary to determine each drug's affinity in the brainstem region.

Another different effect between OLM/AZ and CAN/AM was the speed of BP lowering. Rapid BP reduction causes reflex tachycardia through the activation of the sympathetic nervous system (3,41). A previous study comparing the effects of AZ and AM showed that AZ decreased HR partly due to the slow BP-lowering effect, whereas AM increased HR, despite a similar extent of reduction in BP (41). In this study,

OLM/AZ decreased BP more slowly than CAN/AM, despite a similar powerful extent of reduction in BP after 30 days of treatment, which is a similar BP level of Wistar–Kyoto rats. Thus, the slower BP-lowering effect of OLM/AZ might also contribute to sympathoinhibition observed as a reduction of UNE.

There are some limitations in this study. The effects of combination therapies were not compared with those of each monotherapy, because the aim of this study was to investigate whether there are differences in the antioxidant effect in the brain and the sympathoinhibitory effect between combination therapies using OLM/AZ and CAN/AM in SHRSP with a powerful BP reduction. Further studies are required to evaluate the effects of monotherapies at the same dose as administered in this study to understand the differences in sympathoinhibitory and antioxidant effects, as additive effects, between OLM/AZ and CAN/AM. In this study, a dose of ARB/CCB that is proportional to the dose used in clinical combination therapies was selected because it was considered that the results obtained with these doses would more accurately reflect the effects of the clinical fixed-dose combination therapies. The doses of each drug that are in the range of doses commonly used for the experimental study using hypertensive animals (7,20,42,43) were selected for this study. Finally, this study did not determine whether the combination therapy indeed inhibited sympathetic activity by reducing oxidative stress in the brain. However, it was considered that this mechanism plays an important role in sympathetic control of BP in hypertensive rats as reported in a series of previous studies by the authors themselves and others (8,9,15–18).

In conclusion, the results of this study suggest that chronic oral treatment with OLM/AZ combination and CAN/AM combination, respectively, has a powerful antihypertensive effect and does not elicit baroreflex-mediated sympathetic activation associated with an antioxidant action on the brain in SHRSP. The antioxidant effect on the brain, which is probably due to the action on the brainstem, and the sympathoinhibitory effect of OLM/AZ combination therapy may be greater than those caused using CAN/AM combination therapy.

ACKNOWLEDGEMENTS

This study was supported by Grants-in-Aid for Scientific Research from the Japan Society for the Promotion of Science. The authors are grateful to Daiichi-Sankyo Co. Ltd. for supplying olmesartan medoxomil, azelnidipine, and candesartan cilexetil.

Declaration of interest: The authors report no conflicts of interest. The authors alone are responsible for the content and writing of the paper.

REFERENCES

[1] Mancia G, De Backer G, Dominiczak A, et al. 2007 Guidelines for the management of arterial hypertension: the Task Force for the Management of Arterial Hypertension of the European Society of Hypertension (ESH) and of the European Society of Cardiology (ESC). J Hypertens 2007; 25:1105–1187.

[2] Ogihara T, Kikuchi K, Matsuoka H, et al. The Japanese Society of Hypertension guidelines for the management of hypertension (JSH 2009). Hypertens Res 2009; 32:3–107.

[3] Alderman MH, Cohen H, Roque R, Madhavan S. Effect of long-acting and short-acting calcium antagonists on cardiovascular outcomes in hypertensive patients. Lancet 1997; 349:594–598.

[4] Grassi G. Sympathetic neural activity in hypertension and related diseases. Am J Hypertens 2010; 23:1052–1060.

[5] Ogihara T, Saruta T, Shimada K, Kuramoto K. A randomized, double-blind, four-arm parallel-group study of the efficacy and safety of azelnidipine and olmesartan medoxomil combination therapy compared with each monotherapy in Japanese patients with essential hypertension: the REZALT study. Hypertens Res 2009; 32:1148–1154.

[6] Farsang C, Kawecka-Jaszcz K, Langan J, Maritz F, Zannad F. Antihypertensive effects and tolerability of candesartan cilexetil alone and in combination with amlodipine. Clin Drug Investig 2001; 21:17–23.

[7] Araki S, Hirooka Y, Kishi T, Yasukawa K, Utsumi H, Sunagawa K. Olmesartan reduces oxidative stress in the brain of stroke-prone spontaneously hypertensive rats assessed by an in vivo ESR method. Hypertens Res 2009; 32:1091–1096.

[8] Hirooka Y. Oxidative stress in the cardiovascular center has a pivotal role in the sympathetic activation in hypertension. Hypertens Res 2011; 34:407–412.

[9] Hirooka Y. Role of reactive oxygen species in brainstem in neural mechanisms of hypertension. Auton Neurosci 2008; 142:20–24.

[10] Karas M, Lacourciere Y, LeBlanc AR, et al. Effect of the renin-angiotensin system or calcium channel blockade on the circadian variation of heart rate variability, blood pressure and circulating catecholamines in hypertensive patients. J Hypertens 2005; 23:1251–1260.

[11] Ishizaka T, Takahara A, Iwasaki H, et al. Cardiovascular effects of azelnidipine in comparison with those of amlodipine assessed in the halothane-anaesthetized dog. Basic Clin Pharmacol Toxicol 2010; 106:135–143.

[12] Konno S, Hirooka Y, Araki S, Koga Y, Kishi T, Sunagawa K. Azelnidipine decreases sympathetic nerve activity via antioxidant effect in the rostral ventrolateral medulla of stroke-prone spontaneously hypertensive rats. J Cardiovasc Pharmacol 2008; 52:555–560.

[13] Shokoji T, Fujisawa Y, Kiyomoto H, et al. Effects of a new calcium channel blocker, azelnidipine, on systemic hemodynamics and renal sympathetic nerve activity in spontaneously hypertensive rats. Hypertens Res 2005; 28:1017–1023.

[14] Touyz RM, Briones AM. Reactive oxygen species and vascular biology: implications in human hypertension. Hypertens Res 2011; 34:5–14.

[15] Peterson JR, Sharma RV, Davisson RL. Reactive oxygen species in the neuropathogenesis of hypertension. Curr Hypertens Rep 2006; 8:232–241.

[16] Campos RR. Oxidative stress in the brain and arterial hypertension. Hypertens Res 2009; 32:1047–1048.

[17] Kishi T, Hirooka Y, Kimura Y, Ito K, Shimokawa H, Takeshita A. Increased reactive oxygen species in rostral ventrolateral medulla contribute to neural mechanisms of hypertension in stroke-prone spontaneously hypertensive rats. Circulation 2004; 109:2357–2362.

[18] Chan SH, Wu CW, Chang AY, Hsu KS, Chan JY. Transcriptional upregulation of brain-derived neurotrophic factor

in rostral ventrolateral medulla by angiotensin II: significance in superoxide homeostasis and neural regulation of arterial pressure. Circ Res 2010; 107:1127–1139.

[19] Nozoe M, Hirooka Y, Koga Y, et al. Inhibition of Rac1-derived reactive oxygen species in nucleus tractus solitarius decreases blood pressure and heart rate in stroke-prone spontaneously hypertensive rats. Hypertension 2007; 50:62–68.

[20] Hirooka Y, Kimura Y, Nozoe M, Sagara Y, Ito K, Sunagawa K. Amlodipine-induced reduction of oxidative stress in the brain is associated with sympatho-inhibitory effects in stroke-prone spontaneously hypertensive rats. Hypertens Res 2006; 29: 49–56.

[21] Anzai K, Saito K, Takeshita K, et al. Assessment of ESR-CT imaging by comparison with autoradiography for the distribution of a blood–brain-barrier permeable spin probe, MC-PROXYL, to rodent brain. Magn Reson Imaging 2003; 21:765–772.

[22] Swartz HM, Sentjurc M, Morse II, PD. Cellular metabolism of water-soluble nitroxides: effect on rate of reduction of cell/nitroxide ratio, oxygen concentrations and permeability of nitroxides. Biochim Biophys Acta 1986; 888:82–90.

[23] Takeshita K, Saito K, Ueda J, Anzai K, Ozawa T. Kinetic study on ESR signal decay of nitroxyl radicals, potent redox probes for in vivo ESR spectroscopy, caused by reactive oxygen species. Biochim Biophys Acta 2002; 1573:156–164.

[24] Tanifuji C, Suzuki Y, Geot WM, Horikoshi S, Takahashi H, Tomino Y. Beneficial effects of combination therapy with olmesartan and azelnidipine in murine polycystic kidneys. Kidney Blood Press Res 2009; 32:239–249.

[25] Takai S, Jin D, Shimosato T, Sakonjo H, Miyazaki M. Candesartan and amlodipine combination therapy provides powerful vascular protection in stroke-prone spontaneously hypertensive rats. Hypertens Res 2011; 34:245–252.

[26] Huang BS, Leenen FH. Sympathoinhibitory and depressor effects of amlodipine in spontaneously hypertensive rats. J Cardiovasc Pharmacol 2003; 42:153–160.

[27] Lin Y, Matsumura K, Kagiyama S, Fukuhara M, Fujii K, Iida M. Chronic administration of olmesartan attenuates the exaggerated pressor response to glutamate in the rostral ventrolateral medulla of SHR. Brain Res 2005; 1058:161–166.

[28] Takimoto C, Kumagai H, Osaka M, et al. Candesartan and insulin reduce renal sympathetic nerve activity in hypertensive type 1 diabetic rats. Hypertens Res 2008; 31:1941–1951.

[29] Dampney RA. Functional organization of central pathways regulating the cardiovascular system. Physiol Rev 1994; 74: 323–364.

[30] Tsuchihashi T, Kagiyama S, Matsumura K, Abe I, Fujishima M. Effects of chronic oral treatment with imidapril and TCV-116 on the responsiveness to angiotensin II in ventrolateral medulla of SHR. J Hypertens 1999; 17:917–922.

[31] Kim-Mitsuyama S, Yamamoto E, Tanaka T, et al. Critical role of angiotensin II in excess salt-induced brain oxidative stress of stroke-prone spontaneously hypertensive rats. Stroke 2005; 36:1083–1088.

[32] Masumoto K, Takeyasu A, Oizumi K, Kobayashi T. Studies of novel 1,4-dihydropyridine Ca antagonist CS-905. I. Measurement of partition coefficient (log P) by high performance liquid chromatography (HPLC). Yakugaku Zasshi 1995; 115:213–220.

[33] Cano-Abad MF, Villarroya M, Garcia AG, Gabilan NH, Lopez MG. Calcium entry through L-type calcium channels causes mitochondrial disruption and chromaffin cell death. J Biol Chem 2001; 276:39695–39704.

[34] Lukic-Panin V, Kamiya T, Zhang H, et al. Prevention of neuronal damage by calcium channel blockers with antioxidative effects after transient focal ischemia in rats. Brain Res 2007; 1176:143–150.

[35] Wang JM, Tan J, Leenen FH. Central nervous system blockade by peripheral administration of AT1 receptor blockers. J Cardiovasc Pharmacol 2003; 41:593–599.

[36] Gohlke P, Weiss S, Jansen A, et al. AT1 receptor antagonist telmisartan administered peripherally inhibits central responses to angiotensin II in conscious rats. J Pharmacol Exp Ther 2001; 298:62–70.

[37] Koike H, Sada T, Mizuno M. In vitro and in vivo pharmacology of olmesartan medoxomil, an angiotensin II type AT1 receptor antagonist. J Hypertens Suppl 2001; 19: S3–S14.

[38] Gohlke P, Von Kugelgen S, Jurgensen T, et al. Effects of orally applied candesartan cilexetil on central responses to angiotensin II in conscious rats. J Hypertens 2002; 20: 909–918.

[39] Seltzer A, Bregonzio C, Armando I, Baiardi G, Saavedra JM. Oral administration of an AT1 receptor antagonist prevents the central effects of angiotensin II in spontaneously hypertensive rats. Brain Res 2004; 1028:9–18.

[40] Ueno M, Sakamoto H, Liao YJ, et al. Blood–brain barrier disruption in the hypothalamus of young adult spontaneously hypertensive rats. Histochem Cell Biol 2004; 122: 131–137.

[41] Fujisawa M, Yorikane R, Chiba S, Koike H. Chronotropic effects of azelnidipine, a slow- and long-acting dihydropyridine-type calcium channel blocker, in anesthetized dogs: a comparison with amlodipine. J Cardiovasc Pharmacol 2009; 53:325–332.

[42] Oizumi K, Miyamoto M, Koike H. Effects of dihydropyridine Ca blockers on the renal function in nephrotic spontaneously hypertensive rat (SHR). Biol Pharm Bull 1994; 17: 407–410.

[43] Akasaki T, Ohya Y, Kuroda J, et al. Increased expression of gp91phox homologues of NAD(P)H oxidase in the aortic media during chronic hypertension: involvement of the renin-angiotensin system. Hypertens Res 2006; 29: 813–820.

Articles in PresS. Am J Physiol Cell Physiol (March 28, 2012). doi:10.1152/ajpcell.00068.2012

American Journal of Physiology-Cell Physiology
Regular Research Paper
revised version (redlined article): C-00068-2012R1

Calcium influx through a possible coupling of cation channels impacts skeletal muscle satellite cell activation in response to mechanical stretch

Minako Hara,[1,*] Kuniko Tabata,[1,*] Takahiro Suzuki,[1] Mai-Khoi Q. Do,[1] Wataru Mizunoya,[1] Mako Nakamura,[2] Shotaro Nishimura,[1] Shoji Tabata,[1] Yoshihide Ikeuchi,[1] Kenji Sunagawa,[3] Judy E. Anderson,[4] Ronald E. Allen,[5] and Ryuichi Tatsumi[1]

[1]*Department of Animal and Marine Bioresource Sciences, Graduate School of Agriculture,* [2]*Faculty of Agriculture, Kyushu University, Hakozaki, Fukuoka 8128581, Japan;* [3]*Department of Cardiovascular Medicine, Graduate School of Medicine, Kyushu University, Maedashi, Fukuoka 8128582, Japan;* [4]*Department of Biological Sciences, Faculty of Science, University of Manitoba, Winnipeg, Manitoba R3T 2N2, Canada; and* [5]*Muscle Biology Group, Department of Animal Sciences, College of Agriculture and Life Sciences, University of Arizona, Tucson, Arizona 85721, USA*

Running Head: CALCIUM INFLUX INTO SATELLITE CELLS

---

[*] M. Hara and K. Tabata contributed equally to this work.

Addrress for correspondence: R. Tatsumi, Dept. of Animal and Marine Bioresource Sciences, Graduate School of Agriculture, Kyushu Univ., Hakozaki 6-10-1, Higashi-ku, Fukuoka 812-8581, Japan (e-mail: rtatsumi@agr.kyushu-u.ac.jp).
TEL: +81 92-642-2950; FAX: +81 92-642-2951
APS Regular Member ID[#]: 00060502 (Cell & Molecular Physiology Section)

ABSTRACT

When skeletal muscle is stretched or injured, satellite cells, resident myogenic stem cells positioned beneath the basal lamina of mature muscle fibers, are activated to enter the cell cycle. This signaling pathway is a cascade of events including calcium-calmodulin formation, nitric oxide (NO) radical production by NO synthase, matrix metalloproteinase activation, release of hepatocyte growth factor (HGF) from the extracellular matrix, and presentation of HGF to the receptor c-met, as demonstrated by assays of primary cultures and in vivo experiments. Here, we add evidence that two ion channels, the mechano-sensitive cation channel (MS-channel) and the long-lasting-type voltage-gated calcium-ion channel (L-VGC-channel), mediate the influx of extracellular calcium ions in response to cyclic stretch in satellite-cell cultures. When applied to 1-hr stretch cultures with individual inhibitors for MS- and L-VGC-channels (GsMTx-4 and nifedipine, respectively) or with a less specific inhibitor (gadolinium chloride, Gd), satellite cell activation and upstream HGF release were abolished, as revealed by bromodeoxyuridine-incorporation assays and western blotting of conditioned media, respectively. The inhibition was dose-dependent with a maximum at 0.1 μM (GsMTx-4), 10 μM (nifedipine) or 100 μM (Gd) and cancelled by addition of HGF to the culture media; a potent inhibitor for transient-type VGC-channels (NNC55-0396, 100 μM) did not show any significant inhibitory effect. The stretch response was also abolished when calcium-chelator EGTA (1.8 mM) was added to the medium, indicating the significance of extracellular free calcium ions in our present activation model. Finally, cation/calcium channel dependencies were further documented by calcium-imaging analyses on stretched cells; results clearly demonstrated that calcium ion influx was abolished by GsMTx-4, nifedipine and EGTA. Therefore, these results provide an additional insight that calcium ions may flow in through L-VGC-channels by possible coupling with adjacent MS-channel gating that promotes the local depolarization of cell membranes to initiate the satellite cell activation cascade.

Key Words: Calcium ion influx; Mechano-sensitive channel; Muscle regeneration; Satellite cells; Stretch-activation; Voltage-gated channel

INTRODUCTION

Satellite cells, a population of resident myogenic stem cells positioned between the basal lamina and the sarcolemma of post-natal skeletal muscle fibers, are normally found in a mitotically and metabolically quiescent (or near-dormant) protracted G_1 state (also referred to as G_0) in adult muscles. When muscle is injured, overused, or mechanically stretched, these cells are activated to enter the cell cycle, proliferate to produce large numbers of myoblast progeny, differentiate, and fuse with existing muscle fibers or form new fibers. Through this process, many myonuclei are accumulated in the tissue, and are responsible for increasing protein synthesis and providing the potential to enhance muscle growth (hypertrophy and hyperplasia) and regeneration. Consequently, satellite cell activation is an initial and crucial step in the process of post-natal myogenesis (reviewed in Refs. 12, 28, 45, 50, 66) and may be triggered by mechanical perturbation of satellite cells and muscle fibers. However the detailed mechanism is not fully elucidated.

Of all growth factors studied thus far, including fibroblast growth factors (FGFs), insulin-like growth factor-1 (IGF-1), platelet-derived growth factor BB (PDGF-BB), transforming growth factor-βs (TGF-β1 and 2) and epidermal growth factor (EGF), hepatocyte growth factor (HGF) is the only mitogen with an established ability to stimulate quiescent satellite cells to enter the cell cycle early in primary culture assay and in vivo (1, 58; reviewed in Refs. 15, 38, 72), even though Nagata et al. (40) first demonstrated that sphingosine-1-phosphate (S1P), a bioactive sphingolipid metabolite, induces satellite cells to cycle and very recently Sassoli et al. (48) showed that S1P promotes satellite cell renewal and differentiation in damaged muscle. HGF is a heparin-binding protein localized in the extracellular domain of un-injured skeletal muscle fibers by possible association with glycosaminoglycan chains of proteoglycans, and its predominant form is the active disulfide-linked heterodimer of a 60-kDa α-chain and a 30-kDa β-chain (62). The intracellular signaling receptor for HGF is the c-met proto-oncogene; its message and protein have been found in quiescent and activated satellite cells (1, 19, 58). Thus, release of HGF from its sequestration in the matrix and subsequent presentation to the receptor c-met may be a critical aspect of the activation of quiescent satellite cells. Recently, Wozniak and Anderson (73) provided a novel insight that HGF released from the matrix may induce c-met RNA expression as an immediate-early gene within 30 min in response to muscle fiber stretch and thus enhance HGF-c-met signaling in the satellite-cell activation process.

In a series of previous reports, we employed a FlexerCell system (Flexcell International, Hillsborough, NC) to apply cyclic stretch to isolated rat satellite cells and found that mechanical stretch triggers satellite cell activation by rapidly releasing HGF from its tethering in the extracellular matrix and its subsequent presentation to c-met (59, 60, 63, 65; reviewed in Ref. 66). This phenomenon is relevant to satellite cells in living muscle as revealed by an in vivo muscle-stretch model (64). The most important observation from these previous experiments was that the release of HGF was completely dependent on nitric oxide (NO) radical synthesis by NO synthases (NOS) from L-arginine of the substrate (60, 61). Anderson (4) first pointed to production of NO as a key signal responsible for satellite cell hypertrophy and detachment from the adjacent fiber following crush injury; those results were later verified in in vitro cultures of isolated muscle fibers and their associated satellite cells (5, 6, 71-73; reviewed in Refs. 7, 8). In our subsequent studies, Yamada et al. (75, 76) demonstrated that matrix metalloproteinases (MMPs), a large family of zinc-dependent endopeptidases that collectively degrade one or more extracellular matrix constituents, specifically MMP2, mediate HGF release, possibly by shedding proteoglycan-core proteins in response to the NO radical (reviewed in Refs. 66, 68).

In an effort to understand the events upstream from NO-radical production, recent studies showed that NO-radical/MMP-mediated HGF release and the resulting activation of satellite cells are blocked if calmodulin activity is abolished by the specific inhibitors, calmidazolium, W-13 and W-12; the same report showed that the activation cascade can be turned on when calcium ionophores A23187 or ionomycin are simply added to un-stretched control cultures (67). Therefore, the influx of calcium ions and their binding to calmodulin are thought to be involved in the segment of the activation pathway between sensing the mechanical stimulus and synthesis of the NO radicals, consistent with the observation that the calcium-calmodulin complex associates with constitutive NOS (cNOS: i.e., neuronal and endothelial NOS proteins) to activate NOS enzyme activity, as shown in neuronal and endothelial cells (43, 69). However, it is still unclear how quiescent satellite cells sense mechanical stimuli for transduction into an elevation of the intracellular calcium-ion concentration at the most upstream step of the satellite-cell activation cascade.

Experiments in this study were designed to test the hypothesis that mechano-sensitive cation channels (MS-channels) are involved in the mechano-transduction system. MS-channels are mechanosensing machinery proteins and are widely distributed from single-celled bacteria to animal and plant cells. A variety of experimental approaches

134 revealed that MS-channels respond to a variety of mechanical stimuli, including shear stress,
135 gravity, osmotic pressure and stretch, by opening nanoscale protein pores that are selectively
136 permeable to cations (mainly calcium and sodium) entering into the cytosol down their steep
137 electrochemical gradients (22, 42; reviewed in Refs. 3, 9, 27, 31, 33). Therefore,
138 MS-channel gating may transduce physical stimuli into electrical signals by generating
139 localized depolarization of the cell membranes (through changes in membrane voltage).
140 This depolarization potentially enables the activation of voltage-gated calcium channels
141 (VGC-channels). Indeed, calcium signaling has a central role in regulating activity of many
142 cell types including skeletal muscle fibers in which the long-lasting-type of VGC-channels
143 (L-VGC-channels) in transverse tubules act as a voltage sensor in excitation-contraction
144 coupling (44, 56, 57, 70; reviewed by Refs. 14, 21).
145 In the present paper, we examined the effect of a calcium chelator, EGTA, and
146 selective inhibitors for MS-channels (GsMTx-4) and VGC-channels (nifedipine and
147 NNC55-0396) with and without cyclic stretch of satellite-cell primary cultures on HGF
148 release from the matrix and satellite-cell activation. We provide evidence that extracellular
149 calcium-ion influx through a possible coupling of MS- and L-VGC-channels, may be
150 responsible for the mechano-sensing machinery of quiescent satellite cells.
151
152
153

MATERIALS AND METHODS

Materials. Dulbecco's modified Eagle's medium (DMEM, low glucose type, 31600-034), normal horse serum (HS, 16050-122), antibiotic-antimycotic (15240-062) and gentamicin (15710-064) were purchased from Invitrogen (Grand Island, NY). Poly-L-lysine (P9155), bovine plasma fibronectin (F1141), protease type XIV (P5147) and 5-bromo-2'-deoxyuridine (BrdU, B5002) were obtained from Sigma (St. Louis, MO). Recombinant mouse HGF (2207-HG) was purchased from R&D Systems (Minneapolis, MN). Cation-channel inhibitors, nifedipine (141-05783, 1,4-dihydro-2,6-dimethyl-4-(2-nitrophenyl)-3,5-pyridinedicarboxylic acid dimethyl ester), gadolinium chloride (078-02661) and NNC55-0396 (2268, (1*S*,2*S*)-2-[2-[[3-(1*H*-Benzimidazol-2-yl)propyl] methylamino]ethyl]-6-fluoro-1,2,3,4-tetrahydro-1-(1-methylethyl)-2-naphthalenyl cyclopropanecarboxylate dihydrochloride) were obtained from Wako Pure Chemical Industries (Osaka, Japan), and GsMTx-4 (4393-s, synthetic peptide of the spider venom toxin) was from Peptide Institute (Osaka, Japan).

Fluo3-AM (F026, 1-[2-amino-5-(2,7-dichloro-6-hydroxy-3-oxo-9-xanthenyl) phenoxy]-2-(2-amino-5-methylphenoxy)ethane-*N,N,N',N'*-tetraacetic acid, pentaacetoxymethyl ester) was obtained from Dojindo Laboratories (Kumamoto, Japan). EGTA (15214, *O,O'*-Bis(2-aminoethyl)ethyleneglycol- *N,N,N',N'*-tetraacetic acid) was from Nacalai Tesque (Kyoto, Japan). Calcium ionophore A23187 (21186) and nonionic copolymer surfactant Pluronic F-127 (P2443) were purchased from Sigma.

The following materials were obtained for protein expression analysis: D3 mouse monoclonal anti-desmin and G3G4 mouse monoclonal anti-BrdU antibodies from the Developmental Studies Hybridoma Bank (Iowa City, IA); goat polyclonal anti-human HGF antibody (AB-294-NA) and goat polyclonal anti-c-met antibodies (AF527) from R&D Systems; AC-15 mouse monoclonal anti-β-actin antibody (ab6276) from abcom (Cambridge, MA); horseradish peroxidase (HRPO)-conjugated AffiniPure donkey Anti-goat IgG (705-036-147) from Jackson ImmunoResearch Laboratories (West Grove, PA); affinity-purified biotinylated horse anti-mouse IgG (BA-2000) and the HRPO-labeled avidin kit (PK-6100) from Vector Laboratories (Burlingame, CA); affinity-purified HRPO-conjugated goat anti-mouse IgG (A-4416) and 3,3'-diaminobenzidine (DAB, D5637) from Sigma; HRPO-labeled rabbit anti-goat IgG (414331, Histofine Simple Stain Rat MAX-PO (G)) and normal rabbit serum (426051) from Nichirei BioScience (Tokyo, Japan); Amersham enhanced chemiluminescence (ECL) detection kit (PRN2106),

187 nitrocellulose membrane (Hybond ECL, RPN2020D), and Hyperfilm ECL (28-9068) from
188 GE healthcare (Little Chalfont, UK); and MagicMark XP molecular weight standards
189 (LC5602) from Invitrogen; CanGetSignal immunoreaction solutions (NKB-101) from
190 Toyobo (Osaka, Japan). For the mRNA expression analysis, an RNeasy Micro kit (74004)
191 and QIAshredder homogenizer spin column (79654) from Qiagen (Hilden, Germany),
192 SuperScript III reverse transcriptase (18080-044) from Invitrogen, Oligo-dT primer
193 (H09876) from Roche (Mannheim, Germany), ExTaq DNA polymerase (RR001A) from
194 Takara Bio (Otsu, Japan), agarose-LE (01157) from Nacalai Tesque (Kyoto, Japan), and Gel
195 Red (41000) from Biotium (Hayward, CA) were additionally used.
196
197 ***Animal care and use.*** All experiments involving animals were conducted according to
198 institutional guidelines and with the approval of Kyushu University Institutional Review
199 Board, in collaboration with investigators at the University of Arizona and the University of
200 Manitoba.
201
202 ***Satellite cell isolation and primary culture.*** Satellite cells were isolated from muscle in
203 the hind limb and back of 9-month-old male Sprague-Dawley rats according to Allen et al.
204 (2) with a slight modification (65). Briefly, muscle from the upper hind limb and back
205 were excised, trimmed of fat and connective tissue, minced with scissors, and digested for 1
206 hr at 37°C with 1.25 mg/ml protease type XIV. Cells were separated from muscle-fiber
207 fragments and tissue debris by differential centrifugation and filtration through nylon cell
208 strainers (100 μm and 40 μm mesh size) prior to a final centrifugation step at 1500 x g for 3
209 min, and then plated on poly-L-lysine and fibronectin-coated dishes in DMEM containing
210 10% horse serum (HS), 1% antibiotic-antimycotic mixture, and 0.5% gentamicin
211 (DMEM-10% HS, pH 7.2). Cultures were maintained in a humidified atmosphere of 5%
212 CO_2 at 37°C. In addition, companion satellite-cell cultures, prepared at the same time,
213 were immunostained for the presence of desmin at 30 hr after plating, using a D3
214 monoclonal anti-desmin antibody, biotinylated anti-mouse IgG antibody and HRPO-labeled
215 avidin, in order to determine the percentage of myogenic cells present; cultures with less
216 than 95% DAB-positive cells were not used for experiments.
217 Satellite-cell cultures on Bioflex-Amino silicone-bottom plates (BF-3001A, Flexcell
218 International) were treated with one of the cation-channel inhibitors (GsMTx-4, nifedipine,
219 gadolinium chloride, or NNC55-0396) or a highly selective calcium chelator EGTA (1.8

mM) for 30 min in DMEM-10% HS. GsMTx-4, nifedipine and NNC55-0396 are highly selective peptide/chemical-inhibitors, and are therefore intensely useful for the study of cellular excitability and intracellular calcium-ion signaling and for characterizing effects of therapeutically beneficial drugs. Although detailed inhibitory mechanisms of these compounds still remain unclear, GsMTx-4 selectively inhibits MS-channel activity when applied to the extracellular face of the cell membrane. It does this by increasing the membrane tension required for activation, suggesting that GsMTx-4 acts as a gating modifier (54). By comparison, nifedipine binds directly to inactive L-VGC-channels, which stabilizes their inactive conformation. NNC55-0396 may bind to transmembrane or intracellular domains of the channels to exert their inhibitory effects specifically on transient-type VGC-channels (T-VGC-channels) (29; reviewed in Ref. 53). Cells were then subjected to a cyclic-stretch environment [optimized previously at 25% stretch at 12 sec intervals (59); see Fig. 1 panel *A* for more detail] in a vacuum-operated cyclic strain-providing instrument FlexerCell FX-2000 System (Flexcell International) for 1 hr starting at 24-hr post-plating, as described in the result section with each experiment. In the present study, the stretch periods were all set to 1 hr [half the duration from our original report by Tatsumi et al. (59)] in order to fit calcium-imaging experiments that compare the calcium-influx activity between stretch cultures (in the presence or absence of cation-channel inhibitors or EGTA) and un-stretched control cultures in the same set of experiments within a limited time-period. The stretch-activation activity of satellite cells after 1 hr was not significantly different from that in 2-hr-stretch cultures, as revealed by the BrdU-incorporation assay described below (see Fig. 1 panel *B*, compare *black bars b* and *c*)

Conditioned medium. In experiments in which samples of conditioned media from stretch cultures were assayed by western blotting for the presence of HGF protein released from the cells, cultures were washed with serum-free DMEM at 24-hr post-plating and treatments were imposed for as short as 1 hr in the presence of serum-free DMEM (pH 7.2). The culture medium was supplemented with one of the following for additional treatments: a cation-channel inhibitor GsMTx-4 (0.1 μM), nifedipine (10 μM), or EGTA (1.8 mM) 30 min prior to the addition of cyclic stretch. Conditioned medium from each treatment was collected, centrifuged for 4 min at 1300 x *g*, treated with SDS-sample buffer (2% SDS, 5% β-mercaptoethanol, 10% glycerol, 0.01% bromophenol blue and 62.5 mM Tris-HCl buffer, pH 6.8), and stored at -80°C until use.

253

254 ***In vitro activation assay.*** Cultures were pulse-labeled with 10 μM BrdU in DMEM-10%
255 HS for the final 2 hr from 46 to 48 hr post-plating, followed by immunocytochemistry for
256 detection of BrdU using a G3G4 anti-BrdU monoclonal antibody [1:100 dilution in 0.1%
257 bovine serum albumin (BSA) in phosphate-buffered saline (PBS)] and a HRPO-conjugated
258 anti-mouse IgG antibody (1:500 dilution) according to Tatsumi et al. (58). The percentage
259 of BrdU-labeled cells was used as an indicator of activation and entry into the cell cycle.
260
261 ***Immunoblotting and ECL.*** Mouse recombinant HGF and conditioned media from 1-hr
262 stretch cultures with or without a cation-channel inhibitor or EGTA were applied to 10%
263 polyacrylamide gels for electrophoresis under reducing conditions (35) and transferred to
264 nitrocellulose membranes (58). The blots were blocked with 10% powdered milk in 0.1%
265 polyethylene sorbitan monolaurate (Tween 20)-Tris buffered saline (TTBS) prior to
266 incubation with goat polyclonal anti-HGF antibody (1:500 dilution in 1% powdered
267 milk-TTBS additionally containing 0.05% sodium azide) overnight, and subsequently
268 treated with HRPO-labeled donkey anti-goat IgG antibody at 1:10,000 dilution for 1 hr,
269 followed by ECL detection on Amersham Hyperfilm ECL X-ray film. Internal β-actin in
270 cell lysates was visualized with mouse monoclonal anti-β-actin antibody (1:1,000 dilution
271 in CanGetSignal solution 1, overnight) and with biotinylated horse anti-mouse IgG (1:5,000
272 dilution in CanGetSignal solution 2, for 1 hr) and HRPO-labeled avidin (1:500 dilution in
273 TTBS, for 30 min).
274
275 ***Calcium imaging.*** Satellite-cell cultures on a silicon membrane (11-004-006, Flexcell
276 International) were loaded with 5 μM Fluo3-AM in 0.2% Pluronic F-127 for 1 hr in the dark
277 at 24-hr post-plating, and then rinsed with PBS and left to equilibrate in DMEM-10% HS
278 (pH 7.2) for 60 min at room temperature. Cultures were then exposed to 2-cycles of
279 stretch in the presence of 1.8 mM EGTA or a cation-channel inhibitor (0.1 μM GsMTx-4 or
280 10 μM nifedipine, each added another 30 min prior to the stretch stimulation) under the
281 StageFlexer Jr. system equipped with a 18.5-mm cylindrical loading post; positive-control
282 cells received a calcium ionophore A23187 (3 μM) in the media, according to Tatsumi et al.
283 (67). Calcium images were monitored at intervals of 3 sec under a Nikon ECLIPSE 80i
284 fluorescence microscope system (Tokyo, Japan) with an excitation wavelength of 488 nm
285 and a maximum emission wavelength of 526 nm. Fluorescence intensity was assigned

286 from blue to red in color-coded images by the installed Nikon computer software. After
287 imaging, cells were fixed for 10 min in cold methanol containing 0.1% H_2O_2 and blocked
288 with 5% normal rabbit serum containing 0.6% H_2O_2 in PBS for 20 min. Blocking was
289 followed by immunostaining for the presence of c-met using R&D Systems goat polyclonal
290 primary antibody (1:100 dilution in PBS containing 5% normal rabbit serum) and Histofine
291 Simple Stain HRPO-labeled anti-goat IgG secondary antibody in order to determine if the
292 calcium-imaged cells were myogenic.
293
294 ***Reverse transcription-polymerase chain reaction (RT-PCR).*** Total RNA was purified
295 from cultured satellite cells using an RNeasy Micro kit according to the manufacturer's
296 recommendation. cDNA was synthesized from total RNA by a reverse-transcriptase
297 SuperScript III using oligo-dT primer. PCR was performed using ExTaq DNA polymerase
298 on the mRNA expression of α_{1S}, α_{1C}, α_{1D} and α_{1F} subunits of L-VGC-channels (accession
299 no. NM_053873, NM_012517, NM_017298, and NM_053701, respectively) and transient
300 receptor potential canonical channel (TRPC) 1 and 6 (accession no. NM_053558 and
301 NM_053559, respectively). The intron-spanning primer sets designed by Primer3
302 software were as follows: for rat α_{1S} subunit, forward
303 5'-ACATCTTTGTGGGCTTCGTC-3', reverse 5'-TCCGACTGGTTGTAATGCTG-3',
304 annealing temperature 62°C, amplicon 259 nucleotides (nt); for rat α_{1C} subunit, forward
305 5'-CTCGAAGTTGGGAGAACAGC-3', reverse 5'-GACGAAACCCACGAAGATGT-3',
306 annealing temperature 60°C, amplicon 239 nt; for rat α_{1D} subunit, forward
307 5'-GCAGCACTATGAGCAATCCA-3', reverse 5'-CGGAAAAGACGGAAAAAGGT-3',
308 annealing temperature 60°C, amplicon 249 nt; for rat α_{1F} subunit, forward
309 5'-GCTGCTCAGTAAGGGTGAGG-3', reverse 5'-GTCCTGAAGAGCCACTTTGC-3',
310 annealing temperature 62°C, amplicon 154 nt; for rat TRPC1, forward
311 5'-CGGCAGAATCATTCACACAC-3', reverse 5'-CCAACCCTTCATACCACAGC-3',
312 annealing temperature 57°C, amplicon 215 nt; for rat TRPC6, forward
313 5'-TGAAATTCCTCGTGGTCCTC-3', reverse 5'-GAGCTTGGTGCCTTCAAATC-3',
314 annealing temperature 57°C, amplicon 197 nt. The annealing temperatures and cycle
315 numbers were optimized so that amplification reactions were within the linear range. The
316 PCR products were visualized by 1.5% agarose gel electrophoresis with 0.01% Gel Red
317 reagent.
318

Statistical analysis. Analysis of variance procedures were employed to analyze experimental results using the general linear model procedures of SRISTAT2 for Windows software (Social Survey Research Information, Tokyo, Japan). Least-squares means for each treatment were separated, based on least significant differences. Data were represented as mean and standard error for four cultures per treatment, and statistically significant differences from the mean of control cultures at $p < 0.05$ and $p < 0.01$ were indicated by (*) and (**), respectively. Each experiment was repeated two or three times to verify the reproducibility of results and, in most cases, one rat was used for each experiment.

RESULTS

It is now clear that, in attempting to construct a cascade pathway that translates mechanical perturbation of quiescent satellite cells or muscle fibers into an activation signal, calcium-calmodulin formation is required for NOS activation that produces the NO radical from L-arginine and which subsequently releases HGF from extracellular tethering (for review see Ref. 66). Therefore, the purpose of this study was to clarify a mechanism that responds to mechanical perturbation of stretch by increasing intracellular calcium-ion concentrations in satellite-cell cultures.

The first experiment was designed to examine the significance of extracellular calcium-ion influx in our stretch-activation model of satellite cells in vitro (Fig. 1). Satellite cells were prepared from adult rat skeletal muscles and applied to cyclic-stretch cultures (25% stretch at 12-sec intervals as shown in panel *A*) for 1 hr beginning at 24-hr post-plating in DMEM-10% HS (pH 7.2) with or without 1.8 mM EGTA (calcium chelator that does not enter into the cytosol), followed by the BrdU-incorporation assay at 48-hr post-plating (panel *B*). This concentration of EGTA decreases free calcium ion concentrations in the culture media (1.8 mM) to about 10 μM and without diminishing cell viability, even through the last 24-hr period, as monitored by effects on cell density and BrdU-incorporation at the 48-hr time-point of the assay (*black bar e* and *open bar i*); therefore EGTA was applied to the pilot experiments to determine the dependence of activation on the level of extracellular calcium. Results clearly showed that EGTA treatment abolished stretch-activation (*black bar d*) down to a level equivalent to that in un-stretched control cultures without (*open bar a*) and with 1.8 mM EGTA (*open bar h*). The 1-hr cyclic-stretch cultures (*black bar c*) showed activating activity comparable to cultures receiving 2.5 ng/ml HGF for 24 hr from 24-hr post-plating in the absence or presence of 1.8 mM EGTA (*gray bars f* and *g*, respectively), thereby serving as important controls for other treatment groups in this assay. Together these results provide evidence that extracellular calcium ions are essential in stretch-induced activation of satellite cells in primary culture.

This issue was further examined by studying the effect of cation-channel inhibitors on stretch-activation of satellite cells (Fig. 2 panel *A*). In this experiment, stretch was applied to satellite-cell cultures for 1 hr beginning 24-hr post-plating in the presence of an increasing concentration of one of the selective inhibitors for MS-channels, L-VGC-channels and T-type VGC-channels (0.01-1 μM GsMTx-4, 0.1-10 μM nifedipine and 1-100 μM NNC55-0396, respectively) or a less specific classic-inhibitor for MS-channels (0.1-100 μM gadolinium

364 chloride), and then subsequently assayed for satellite-cell activation at 48-hr post-plating as
365 described previously. The T-VGC-channel inhibitor NNC55-0396 (*open square*) did not
366 show a significant effect on activation in the range examined here or in another report (29, 55).
367 Exposures to one of the other three cation-channel inhibitors all abolished stretch-stimulated
368 activation in a dose-dependent manner. GsMTx-4 (*closed circle*) was the most powerful of
369 the three inhibitors, with blocking at an optimal concentration of 0.1 μM versus 10 μM for
370 nifedipine (*closed square*) and 100 μM for Gd (*open circle*). None of these cation-channel
371 inhibitors diminished cell viability, again as monitored at 48-hr by cell density and in
372 comparison to the BrdU-labeling of control cultures receiving cation-channel inhibitors (*open*
373 *bars h-j*), and by results showing that addition of HGF (2.5 ng/ml) to individual-inhibitor
374 cultures (*gray bars d-g*) stimulated satellite cell activation to a level equivalent to HGF (*gray*
375 *bar c*) and stretch (*black bar b*). These observations, therefore, indicated that both MS- and
376 L-VGC-channels are essential in the stretch activation of satellite cells and may be mediating
377 the influx of extracellular calcium ions in response to mechanical stretch. Also, as shown in
378 Fig. 2 panel *B*, the implication of MS- and L-VGC-channels in the activation cascade was
379 further emphasized by western blot detection of the 60 kDa α-chain of HGF in conditioned
380 media (serum-free DMEM, pH 7.2); media were collected from the 1-hr stretch cultures that
381 had received the optimal dose of GsMTx-4 (0.1 μM), nifedipine (10 μM), or EGTA (1.8 mM)
382 and assayed for HGF. Results qualitatively demonstrated that the cyclic stretch culture
383 stimulates HGF release (consistent with our original results) (*lane m*), and even in the
384 presence of stretch, GsMTx-4 (*lane n*), nifedipine (*lane o*) and EGTA (*lane p*) diminish
385 release of HGF with an apparently similar potency. This indicates that HGF release from
386 extracellular matrix depends on the up-stream MS- and L-VGC-channel activities. In fact,
387 the messages of α_{1S} and α_{1C} subunits of L-VGC-channels were detected by RT-PCR analysis
388 for satellite cells at 24-hr post-plating, which is the time at which the stretch treatment was
389 applied in the present and our previous experiments (65, 75-77) (Fig. 3 panel *A*). Because
390 L-VGC-channel proteins are now classified into $Ca_{v1.1}$, $Ca_{v1.2}$, $Ca_{v1.3}$ and $Ca_{v1.4}$ according to
391 their corresponding α_1-subunits, α_{1S}, α_{1C}, α_{1D} and α_{1F} (34, 36), our PCR results indicate that
392 $Ca_{v1.1}$ and $Ca_{v1.2}$ may exist in quiescent satellite cells and be responsible for calcium ion influx
393 by coupling with MS-channel gating that senses mechanical perturbation of satellite cells.
394 Finally in a series of extracellular calcium ion dependency experiments, calcium ion
395 influx was documented by analysis of calcium imaging studies for two-cycle stretched
396 satellite cells at 24-hr post-plating in the presence or absence of cation-channel inhibitors (Fig.

4). Calcium ionophore treatment (3 μM A23187, without stretch or treatment with channel inhibitors) stimulated increase in intracellular calcium ion concentrations, consistent with our previous result (67) and therefore served as a positive control within this assay (*row A*). Cyclic stretch also affects calcium ion influx as shown in *row B*, in which the fluorescence intensity reached a maximum at 30-60 sec post-stretch and the calcium signal maintained a plateau within at least 210 sec (far-right image) and typically 300 sec of the maximum recording time-point of the present analysis (image not shown), and that response was almost abolished to reach a level comparable to 1.8 mM EGTA-treated cultures when stretch cultures received 0.1 μM GsMTx-4 or 10 μM nifedipine (*rows C* and *D*, respectively). These observations provide direct evidence that both MS- and L-VGC-channels are essential in mediating the extracellular calcium ion influx in response to mechanical stretch in skeletal muscle satellite cells in culture.

DISCUSSION

The importance of satellite cell proliferation activity in skeletal muscle repair and hypertrophy has been appreciated for a considerable time. It is well documented that one of the earliest events, triggering the activation of quiescent satellite cells, is initiated by mechanical or chemical stimuli and enables satellite cells to migrate and enter the cell proliferation cycle. Bischoff (11) was among the first to explore the biochemical link between satellite cell activation and mechanical perturbation of muscle tissue. His classical experiments used a crushed-muscle extract, which he found could stimulate satellite cells associated with isolated fibers to synthesize DNA and divide. Johnson and Allen (30) later reported that the same crushed-muscle extract could stimulate adult rat satellite cells in culture to enter the cell cycle earlier than adult rat cultures in control medium. Shortening of the lag phase observed with freshly isolated adult satellite cells has since been used as an assay for satellite cell activation (1, 2, 58) and this assay was employed in experiments that first demonstrated that HGF was unique in its ability to activate satellite cell division in vitro (1). In subsequent experiments, the active agent in crushed-muscle extract was shown to be HGF, which was present in un-injured muscle and located primarily in the extracellular matrix (58, 62). In further experiments, Tatsumi et al. (59-61, 64) showed that satellite cells were stimulated to enter the cell cycle when subjected to mechanical stretch in primary culture and living muscle. We also demonstrated that satellite cell activation was due to rapid release of HGF from its extracellular tethering and the subsequent presentation to the receptor c-met, and later verified that HGF release is dependent on calcium-calmodulin formation and the down-stream NO radical-mediated activation of matrix metalloproteinases (MMPs) (47, 67, 75, 76).

These observations suggest that the stretch-activation of satellite cells is a cascade of sequential events including (in order) an influx of calcium ions and their binding to calmodulin, NO radical production by cNOS, MMP activation, HGF release from the matrix and presentation of HGF to the signaling receptor c-met (see a review of Ref. 66). In this model, a complex of HGF and proteoglycan extracellular domain would be shed from the matrix and presented to the receptor c-met. In fact, HGF associated with heparan sulfate moieties has a greater affinity for c-met relative to HGF alone, and therefore, has enhanced HGF signaling activity (20). Such a complex has been detected in PBS extracts from crushed muscle and intact muscle incubated in the NO donor, sodium nitroprusside (SNP) (Allen et al., unpublished data), supporting the above insight. In related experiments by